ELSEVIER

New cation-dependent supramolecular arrangements of [RTeI$_4$]$^-$ tectons: Synthesis and X-ray structural characterization of the mixed valence complex salts [p-CH$_3$O(C$_6$H$_4$)Te(etu)]-[p-CH$_3$O(C$_6$H$_4$)TeI$_4$] (etu = ethylenethiourea) and [p-PhO(C$_6$H$_4$)Te(tu)][p-PhO(C$_6$H$_4$)TeI$_4$] (tu = thiourea)

Gleison Antônio Casagrande [a], Ernesto Schulz Lang [a,*], Gelson Manzoni de Oliveira [a,*], Sebastião S. Lemos [b], Viviane A.S. Falcomer [b]

[a] *LMI – Departamento de Química, Universidade Federal de Santa Maria, 97.105-900 Santa Maria, RS, Brazil*
[b] *Instituto de Química, Universidade de Brasília, 70904-970, Brasília, DF, Brazil*

Abstract

(p-CH$_3$OC$_6$H$_4$Te)$_2$ and (p-PhOC$_6$H$_4$Te)$_2$ react with I$_2$ and thiourea/ethylenethiourea to give the mixed valence complex salts [p-CH$_3$O(C$_6$H$_4$)Te(etu)][p-CH$_3$O(C$_6$H$_4$)TeI$_4$] (**1**) and [p-PhO(C$_6$H$_4$)Te(tu)][p-PhO(C$_6$H$_4$)TeI$_4$] (**2**). Both compounds confirm the tectonic character of the tetraiodo-organyltellurates [RTeI$_4$]$^-$ with the assembling of polymeric chains of [p-CH$_3$O(C$_6$H$_4$)TeI$_4$]$_2^{2-}$ and [p-PhO(C$_6$H$_4$)TeI$_4$]$_2^{2-}$ dimers linked through single (**1**) and double (**2**) I$\cdots$I secondary bonds. The strong covalent character of the cation–anion interaction of **2** allows its further representation as the mixed valence molecular species [RTeI$_3$(μ-I)Te(tu)R] {R = p-PhO(C$_6$H$_4$)}.
© 2006 Elsevier B.V. All rights reserved.

Keywords: Organotellurium halides; Tectonic tetraiodo-organyltellurates; Supramolecular assembling of [RTeI$_4$]$^-$ ions

1. Introduction

If we consider Simard's *tecton* (from Greek, *tekton*, builder) definition [1] – any molecule whose interactions are dominated by particular associative forces that induce the self-assembly of an organized network with specific architectural or functional features – and the concept of supramolecular synthesis [2,3], then the species [RTeX$_4$]$^-$ (R = aryl; X = halogen) surely play an important role in this chemical field, due to their remarkable ability to act as supermolecule-building tectons. We have already described some examples with this tendency: initially we

have found [4] three different packing arrangements in the crystal lattice of [PhTeCl$_4$]$^-$ salts, all of them arising from secondary Te$\cdots$Cl bonds (which complete the octahedral coordination at tellurium) and hydrogen–halogen bonds between the anion and the stabilizing cations (pyridonium, for example). When the same, not too bulky cationic species is maintained for different – and bigger – [PhTeX$_4$]$^-$ (X = Br, I) anions, the polymerization gradually increases substantially [5]. Further, in the lattice of {Cs[PhTeCl$_4$]·CH$_3$OH]} and Cs[PhTeBr$_4$] the alkali metal cation interacts secondarily with the chlorine and bromine Te-ligands holding the structures in tridimensional, supramolecular assemblies [6]. In tetraiodo-organyltellurates stabilized by cations without acid N–H functions such as (Et$_4$N)[PhTeI$_4$] and (Et$_4$N)[(β-naphthyl)TeI$_4$], only the Te$\cdots$I and I$\cdots$I secondary bonds behave as structure-

forming interactions in the self-organization of the supra-ionic lattices [7] which are also strongly dependent on the size of the organic group.

Another interesting characteristic of $[RTeX_4]^-$ anions is their trend to be also stabilized by Se^{II} and Te^{II} cation complexes to form mixed valence complex salts. We have newly reported some structures of this kind of complexes, such as $[PhSe(tu)][PhTeI_4]$, $[PhSe(tu)][PhTeBr_4]$ [8] and $[Ph(etu)-Te(\mu-I)Te(etu)Ph][PhTeI_4]$ [9]. In these cases, however, the tectonic character of the $[RTeX_4]^-$ ion – e.g., its ability to build supermolecules through secondary interactions – is very limited, probably due to the stereochemical effects associated with the size of the cation complex. Thus, in $[PhSe(tu)][PhTeI_4]$ there occurs dimeric association of anionic $[PhTeI_4]^-$ through reciprocal Te···I interactions, with the participation of two $[PhSe(tu)]^+$ cationic moieties through Se···I interactions. Dimeric assembling and strong covalent cation-anion interactions were also observed in the "molecular" complexes described in the same report [8], $[(tmtu)PhTe(\mu-Br)TeBr_3Ph]_2$ and $[(tu)PhTe(\mu-I)TeI_3Ph]_2$ (tmtu = tetramethylthiourea); on the other hand, in $[PhSe-(tu)][PhTeBr_4]$ (of the same series), the tectons $[PhTeBr_4]^-$ are able to achieve a very complex (zigzag) polymeric chain, additionally reinforced by three secondary bonds of cationic selenium atoms to the bromine ligands of the surrounding anionic units. Finally, in the lattice of $[Ph(etu)-$ $Te(\mu-I)Te(etu)Ph][PhTeI_4]$ [9], there are no cation–anion interactions, and the anions $[PhTeI_4]^-$ appear merely in dimeric association through symmetrical and reciprocal Te···I interactions, which accomplish the octahedral configuration of the Te centres.

In the light of these experimental studies we now report on the synthesis and the structural characterization of the new mixed valence complex salts $[p-CH_3O(C_6H_4)-Te(etu)][p-CH_3O(C_6H_4)TeI_4]$ (1) and $[p-PhO(C_6H_4)-Te(tu)][p-PhO(C_6H_4)TeI_4]$ (2), where the Te^{IV} anions $[p-CH_3O(C_6H_4)TeI_4]^-$ and $[p-PhO(C_6H_4)TeI_4]^-$ confirm their tectonic character. In both compounds the anions are linked in the well known dimeric association through reciprocal Te···I secondary interactions which assure the octahedral coordination of the Te atoms. Single I···I interactions in 1 generate a polymeric chain, in 2 the dimers are linked through double I···I bonding in a curious polymeric conformation. The strong cation–anion interaction in 2 also allows its molecular representation.

2. Experimental

All manipulations were conducted under nitrogen by the use of standard Schlenk techniques. Methanol was dried with Mg/I_2 and distilled before use [10]. The respective ditellurides were prepared according literature procedures [11].

Table 1
Crystal data and structure refinement for 1 and 2

	1	2
Empirical formula	$C_{17}H_{20}I_4N_2O_2STe$	$C_{50}H_{44}I_8N_4O_4S_2Te_4$
Formula weight	1079.21	2354.61
T (°K)	273(2)	296(2)
Radiation, λ (Å)	0.71	0.71
Crystal system, space group	Triclinic, $P\bar{1}$	Triclinic, $P\bar{1}$
Unit cell dimensions		
a (Å)	8.9778(2)	13.7100(3)
b (Å)	10.1681(2)	13.7489(2)
c (Å)	15.4585(4)	18.3665(3)
α (°)	74.7630(10)	69.2470(10).
β (°)	85.3610(10)	81.4250(10)
γ (°)	89.5750(10)	79.4890(10)
V (Å^3)	1356.96(5)	3169.63(10)
Z, Calculated density (g cm^{-3})	2, 2.641	2, 2.467
Absorption coefficient (mm^{-1})	6.792	5.827
$F(000)$	968	2136
Crystal size (mm)	$0.24 \times 0.14 \times 0.04$	$0.12 \times 0.11 \times 0.09$
θ Range (°)	1.37–30.87	1.19–28.38
Index ranges	$-12 \leqslant h \leqslant 12,$	$-17 \leqslant h \leqslant 18,$
	$-14 \leqslant k \leqslant 14,$	$-18 \leqslant k \leqslant 18,$
	$-22 \leqslant l \leqslant 22$	$-24 \leqslant l \leqslant 24$
Reflections collected	45,165	62,531
Reflections unique	8454 [$R_{int} = 0.0279$]	15834 [$R_{int} = 0.0258$]
Completeness to theta max.	98.8%	99.6%
Absorption correction	Semi-empirical	Semi-empirical
Max. and min. transmission	0.7728 and 0.2925	0.6221 and 0.5415
Refinement method	Full-matrix least-squares on F^2	Full-matrix least-squares on F^2
Data/restraints/parameters	8454/0/253	15834/0/649
Goodness-of-fit on F^2	1.161	1.118
Final R indices [$I > 2\sigma(I)$]	$R_1 = 0.0261, wR_2 = 0.0811$	$R_1 = 0.0276, wR_2 = 0.0759$
R indices (all data)	$R_1 = 0.0415, wR_2 = 0.1004$	$R_1 = 0.0479, wR_2 = 0.0982$
Largest diff. peak and hole (e Å^{-3})	1.695 and -1.280	1.664 and -1.481

2.1. [p-CH₃O(C₆H₄)Te(etu)] [p-CH₃O(C₆H₄)TeI₄] (1)

To a solution of 0.047 g (0.1 mmol) of (p-CH₃OC₆H₄Te)₂ - dianisylditelluride - in 30 ml of methanol, 0.0253 g (0.1 mmol) of resublimed I₂ were added. After stirring for 2 min, to the p-CH₃OC₆H₄TeI solution 0.0204 g (0.2 mmol) of ethylenethiourea was added and the black color turned red instantaneously {formation of the Te^{II} intermediary p-CH₃OC₆H₄Te(etu)I}. To the red mixture 0.123 g (0.2 mmol) of p-CH₃OC₆H₄TeI₃ was added and the solution was refluxed mildly at 50 °C for 1 h. After cooling at room temperature the mixture was filtered and the slow evaporation of the solvent gave black-reddish crystals of the product.

Properties: air stable, black-reddish crystalline substance; C₁₇H₂₀I₄N₂O₂STe (1079.21). Yield: 83% based on (p-CH₃OC₆H₄Te)₂; Melting point: 118–120 °C; C, H, N-analysis: Calc.: C, 18.92; H, 1.87; N, 2.60. Found: C, 18.79; H, 1.62; N, 2.65%.

2.2. [p-PhO(C₆H₄)Te(tu)] [p-PhO(C₆H₄)TeI₄] (2)

To a red solution of 0.1186 g (0.2 mmol) of (p-PhOC₆H₄Te)₂ – diphenoxyphenylditelluride – in 30 ml of methanol, 0.0506 g (0.2 mmol) of resublimed I₂ was added and the color turned black. After the addition of 0.0152 g (0.2 mmol) of thiourea and supplementary 0.0506 g (0.2 mmol) of resublimed I₂ the temperature was kept at 40 °C for 40 min. At room temperature the mixture was fil-

tered. The slow evaporation of the solvent yielded black-reddish crystals.

Properties: air stable black-reddish crystals; C₅₀H₄₄I₈N₄O₄S₂Te₄ (2354.61). Yield: 65% based on (p-PhOC₆H₄Te)₂; Melting point: 125–127 °C; C, H, N-analysis: Calc.: C, 25.86; H, 1.91; N, 2.41. Found: C, 25.92; H, 1.80; N, 2.59%.

Table 2
Selected bond lengths [Å] and angles [°] for **1**

Bond lengths	
Te(1)–C(11)	2.144(4)
Te(1)–I(3)	2.8741(4)
Te(1)–I(4)	2.9303(4)
Te(1)–I(2)	2.9679(4)
Te(1)–I(1)	3.0251(4)
Te(1)···I(2)#1	3.7800(4)
I(3)···I(3)#1	3.6660(6)
Te(2)–C(21)	2.114(4)
Te(2)–S(1)	2.5163(14)
Te(2)···I(3)	4.1772(4)
Bond angles	
C(11)–Te(1)–I(3)	90.85(11)
C(11)–Te(1)–I(4)	4.42(12)
I(3)–Te(1)–I(4)	89.587(12)
C(11)–Te(1)–I(2)	93.59(12)
C(11)–Te(1)···I(2)#1	169.74(12)
I(3)–Te(1)–I(2)	90.409(11)
I(4)–Te(1)–I(2)	171.990(13)
C(11)–Te(1)–I(1)	89.48(11)
I(3)–Te(1)–I(1)	175.146(13)
I(4)–Te(1)–I(1)	85.559(12)
I(2)–Te(1)–I(1)	94.404(11)
I(2)–Te(1)···I(2)#1	78.55(1)
C(21)–Te(2)–S(1)	92.19(12)
C(21)–Te(2)···I(3)#1	160.41(11)
S(1)–Te(2)···I(3)#1	74.70(3)

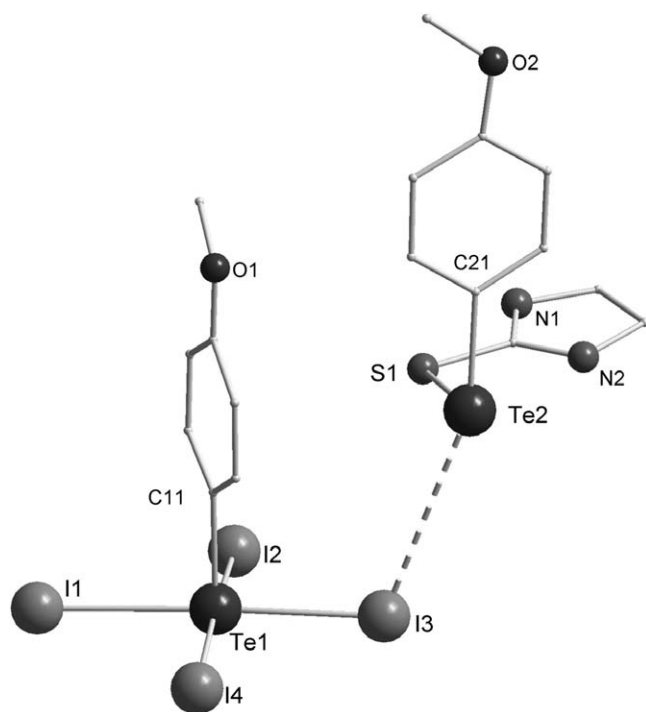Symmetry transformations used to generate equivalent atoms: #1 −x + 2, −y + 1, −z + 1.

Table 3
Selected bond lengths [Å] and angles [°] for **2**

Bond lengths	
C(11)–Te(1)	2.148(4)
S(1)–Te(3)	2.4895(18)
Te(1)–I(1)	3.0750(4)
Te(1)–I(2)	2.8672(5)
Te(1)–I(3)	2.8371(4)
Te(1)–I(4)	3.0151(4)
Te(1)···I(4)#1	3.8422(5)
Te(2)–I(7)	2.8785(5)
Te(2)–I(6)	2.9177(4)
Te(2)–I(8)	2.9607(5)
Te(2)–I(5)	2.9661(4)
Te(2)···I(5)#2	3.654(2)
I(1)···Te(3)	3.3000(6)
I(6)···Te(4)	3.4315(6)
I(3)#1···I(5)#1	3.637(2)
I(1)···I(7)#1	4.0595(5)
I(3)···I(5)	3.6367(5)
I(1)#1···I(7)#2	4.0595(5)
Bond angles	
C(11)–Te(1)–I(3)	92.69(12)
C(11)–Te(1)–I(2)	92.35(12)
I(3)–Te(1)–I(2)	91.031(15)
C(11)–Te(1)–I(4)	90.49(12)
I(3)–Te(1)–I(4)	88.328(13)
I(2)–Te(1)–I(4)	177.112(15)
C(11)–Te(1)–I(1)	89.26(12)
I(3)–Te(1)–I(1)	177.306(14)
I(2)–Te(1)–I(1)	87.028(14)
I(4)–Te(1)–I(1)	93.519(13)
C(11)–Te(1)···I(4)#1	171.09(12)
I(3)–Te(1)···I(4)#1	91.854(11)
I(2)–Te(1)···I(4)#1	79.902(12)
I(4)–Te(1)···I(4)#1	97.302(11)
I(1)–Te(1)···I(4)#1	85.969(11)
Te(1)–I(4)···Te(1)#1	82.70(1)
C(31)–Te(2)–I(5)	90.31(12)
C(31)–Te(2)–I(7)	92.82(12)
C(31)–Te(2)–I(6)	93.60(12)
C(31)–Te(2)–I(8)	90.95(12)
I(7)–Te(2)–I(6)	90.186(14)
I(7)–Te(2)–I(8)	89.478(15)
I(6)–Te(2)–I(8)	175.441(14)
I(7)–Te(2)–I(5)	175.167(16)
I(6)–Te(2)–I(5)	93.295(13)
I(8)–Te(2)–I(5)	86.786(14)
C(31)–Te(2)···I(5)#2	178.11(14)
I(5)–Te···I(5)#2	88.14(1)
I(7)–Te(2)···I(5)#2	88.66(1)
I(6)–Te(2)···I(5)#2	93.295(13)
I(8)–Te(2)···I(5)#2	86.786(14)
Te(2)–I(5)···Te(2)#2	91.860(12)

Symmetry transformations used to generate equivalent atoms: #1 −x + 1, −y, −z + 1; #2 −x, 1 − y, 1 − z.

Fig. 1. Asymmetric unit of [p-CH₃O(C₆H₄)Te(etu)][p-CH₃O(C₆H₄)TeI₄] (1). The dashed line identifies the secondary interaction.

2.3. Crystallography

X-ray data were collected on a Bruker SMART CCD diffractometer. The crystallographic structures of [p-CH₃O(C₆H₄)Te(etu)][p-CH₃O(C₆H₄)TeI₄] (**1**) and [p-PhO(C₆H₄)Te(tu)][p-PhO(C₆H₄)TeI₄] (**2**) were solved by direct methods (SHELXS-97) [12]. Refinements were carried out with the SHELXL-97 [13] package. All refinements were made by full-matrix least-squares on F^2 with anisotropic displacement parameters for all non-hydrogen atoms. Hydrogen atoms were included in the refinement in calculated positions.

2.4. ^1H, ^{13}C, and ^{125}Te NMR

The NMR spectral data were obtained in a Varian Mercury Plus 7.05 T spectrometer with 300.07 MHz (^1H), 75.46 MHz (^{13}C) and 94.74 MHz (^{125}Te). The samples were dissolved in a 9:1 mixture of acetone-d₆ and DMSO-d₆, respectively. The solutions were measured in NMR tubes of 5 mm, at 300 °K. The ^1H NMR and ^{13}C NMR chemical shifts are relative to Si(CH₃)₄ as internal reference. The ^{125}Te NMR spectra were taken with reference to (CH₃)₂Te. A capillary containing Ph₂Te₂ dissolved in CDCl₃ (δ 450) was used as external reference.

3. Results and discussion

The crystal data and experimental conditions are given in Table 1. Selected bond distances and angles of [p-CH₃O(C₆H₄)Te(etu)][p-CH₃O(C₆H₄)TeI₄] (**1**) and [p-PhO(C₆H₄)Te(tu)][p-PhO(C₆H₄)TeI₄] (**2**) are listed in Tables 2 and 3, with dashed lines representing the secondary bonds. Figs. 1 and 3 display the asymmetric units of compounds **1** and **2**, with the secondary interactions also identified by dashed lines. Fig. 2 represents the dimeric association of the anions [p-CH₃O(C₆H₄)TeI₄]⁻ in compound **1** and their polymeric assembling through single I···I secondary bonds. Fig. 4 shows the dimerization of the [p-PhO(C₆H₄)TeI₄]⁻ anions of **2** and the attainment of a polymeric chain through double I···I secondary interactions. The significant long interionic distance {Te(2)···I(3) = 4.1772(4) Å, see Fig. 1} in [p-CH₃O(C₆H₄)-Te(etu)][p-CH₃O(C₆H₄)TeI₄] (**1**) and consequently the weak cation–anion interaction should exclude the possibility to represent this compound in a molecular way, such as [RTeI₃(μ-I)Te(etu)R]₂ {R = p-CH₃O(C₆H₄)}, for example. In [p-PhO(C₆H₄)Te(tu)][p-PhO(C₆H₄)TeI₄] (**2**) there occurs a strong cation–anion interaction {I(1)···Te(3) = 3.3000(6), I(6)···Te(4) = 3.4315(6) Å} (see Fig. 3); therefore, and according to previous results [8], the representation of the
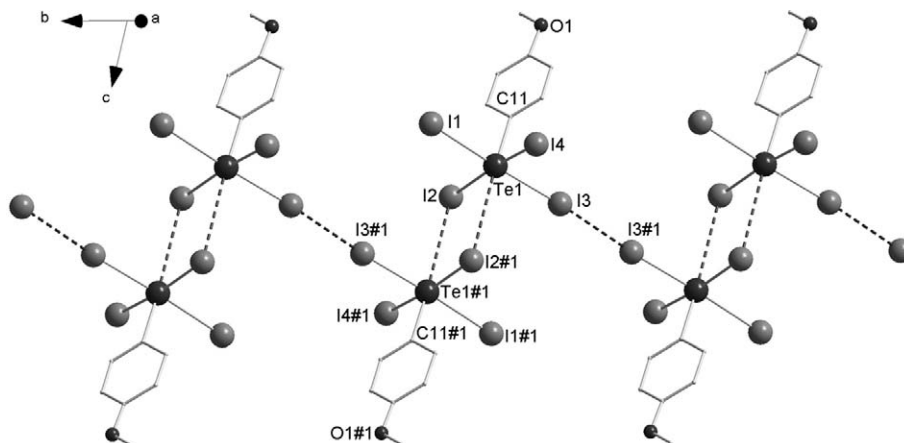

Fig. 2. Dimeric association of the anions [p-CH₃O(C₆H₄)TeI₄]⁻ in compound **1** and their polymeric assembling along the b axis through I–I secondary interactions (dashed lines). Symmetry transformations used to generate equivalent atoms: #1 −x + 2, −y + 1, −z + 1.
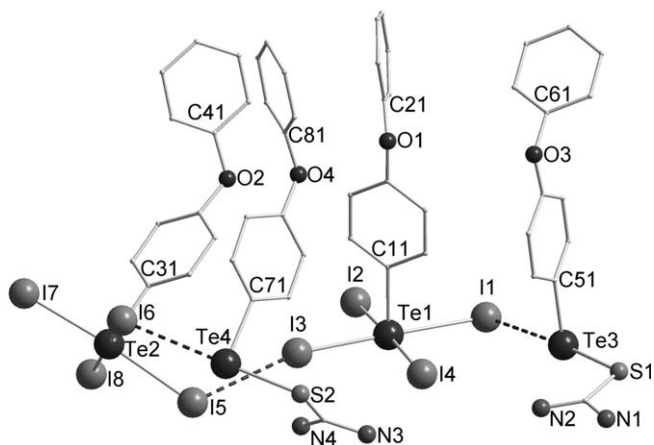
Fig. 3. Asymmetric unit of $[RTeI_3(\mu\text{-}I)Te(tu)R]$ $\{R = p\text{-}PhO(C_6H_4)\}$. Secondary interactions and bonds as dashed lines.

mixed valence complex salt $[p\text{-}PhO(C_6H_4)Te(tu)][p\text{-}PhO(C_6H_4)TeI_4]$ (2) which corresponds to the real (molecular) atomic aggregation of the compound would be $[RTeI_3(\mu\text{-}I)Te(tu)R]$ $\{R = p\text{-}PhO(C_6H_4)\}$. This spell way does not exclude the dimerization tendency of the $[RTeI_4]$ moieties, where the reciprocal $Te\cdots I$ secondary bonds measure 3.8422(5) Å $\{Te(1)\cdots I(4)\#1\}$, somewhat longer than the equivalent distances observed in compound 1 $\{Te(1)\cdots I(2)\#1 = 3.7800(4)$ Å$\}$.

In both compounds the tectonic character of the $RTeI_4$ moieties is remarkably strong. The $I\cdots I$ (secondary) distances of the dimers $[p\text{-}CH_3O(C_6H_4)TeI_4]_2^{2-}$ in 1 is 3.6660(6) Å $\{I(3)\cdots I(3)\#1\}$. In compound 2 the supramolecular tectonic assembling of the type $[RTeI_3(\mu\text{-}I)\text{-}Te(tu)R]_n$ $\{R = p\text{-}PhO(C_6H_4)\}$ is achieved through double, asymmetric $I\cdots I$ secondary interactions (see Fig. 4): $I(3)\#1\cdots I(5)\#1 = 3.637(2)$, $I(1)\cdots I(7)\#1 = 4.0595(5)$, $I(3)\cdots I(5) = 3.6367(5)$ and $I(1)\#1\cdots I(7)\#2 = 4.0595(5)$ Å.
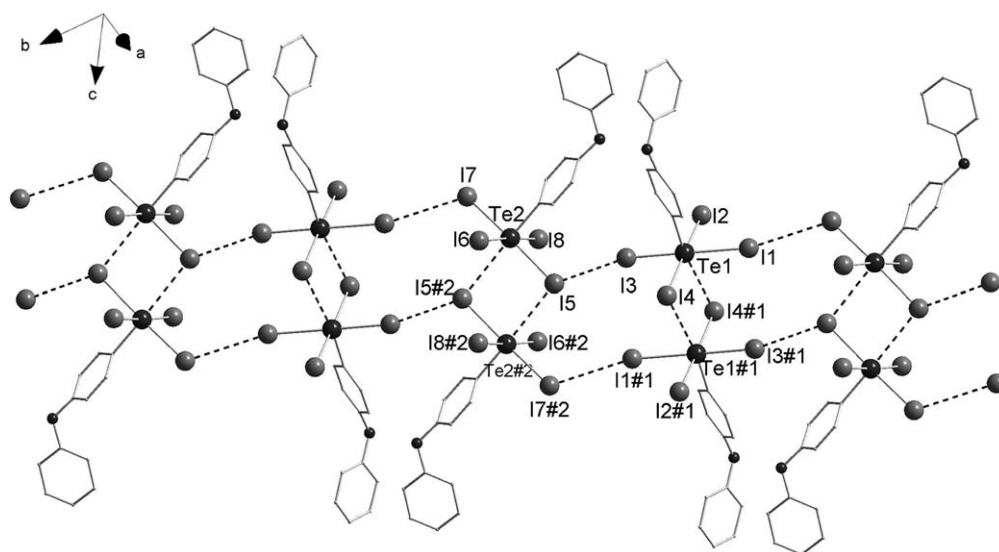
This asymmetry is evident in the apparent irregular contour of the chain, which, despite this, shows in the middle of the Te(1)–Te(1)#1 dimers inversion centres which, respectively, enclose the two neighbored dimers, achieving vicinal sequences of 12-atom rings.

Attempts to study the dissociation of the title complexes in solution by means of multinuclear NMR spectra were limited by the fact that the crystals of 1 and 2 are soluble only in coordinating solvents like dimethylsulfoxide (DMSO). Another limiting factor represents the occurrence of dynamic equilibrium in solution due to the exchange between ligand and solvent molecules, predominantly with DMSO. To minimize this effect ^1H, ^{13}C, and ^{125}Te NMR studies were conducted in solutions of acetone-d_6 and DMSO-d_6 in a 9:1 proportion, respectively. Complex 1 gives a ^{125}Te NMR broad signal at 933.5 ppm, 2 generates a wide peak localized in 894.6 ppm. The ^1H and ^{13}C NMR signals of compounds 1 and 2 are: ^1H NMR 1: 8.93 (broad, 2N–H), 8.25 (d, 4C–H$_{arom.}$), 6.81 (d, 4C–H$_{arom.}$), 3.90 (s, 4H CH$_2$ etu), 3.82 ppm (s, 6H CH$_3$–O–); 2: 8.5 (broad, 4H N–H), 6.8–7.5 ppm (multiplet, 18H$_{arom.}$). ^{13}C NMR 1: 176.3 (C=S), 160.89 (C4), 143.95 (C2 and C6), 115.3 (C3 and C5), 108.6 (s, weak, C_1–Te), 55.56 (CH$_3$–O–), 46.3 ppm (2CH$_2$ etu); 2: 171.0 (C=S), whole aromatic signals 158.6, 157.9, 156.8, 144.3, 140.3, 130.9, 130.7, 130.6, 124.7, 124.0, 120.6, 120.2, 119.4, 119.3, 118.8 ppm, 112.07 ppm (s, weak, C_1–Te).

4. Supplementary material

Crystallographic data for the structural analyses have been deposited with the Cambridge Crystallographic Data Centre CCDC nos. CSD 609607 and 609608 for compounds 1 and 2. Further details of the crystal structure investigations are available free of charge via www.ccdc. cam.ac.uk/conts/retrieving.html (or from the CCDC, 12

Fig. 4. Supramolecular lattice of $[RTeI_3(\mu\text{-}I)Te(tu)R]_n$ $\{R = p\text{-}PhO(C_6H_4)\}$; for clarity only the $[p\text{-}PhO(C_6H_4)TeI_4]$ dimers are represented. Secondary interactions in dashed lines. Symmetry transformations used to generate equivalent atoms: #1 $-x + 1$, $-y$, $-z + 1$; #2 $-x$, $1 - y$, $1 - z$.

Union Road, Cambridge CB2 1EZ, UK; fax: +44 1223 336033; e-mail: deposit@ccdc.cam.ac.uk).

References

[1] S. Simard, D. Su, J.D. Wuest, J. Am. Chem. Soc. 113 (1991) 4696.
[2] M.C.T. Fyfe, J.F. Stoddart, Acc. Chem. Res. 30 (1997) 393.
[3] J.-M. Lehn, Supramolecular Chemistry, VCH, Weinheim, 1995.
[4] E. Schulz Lang, R.M. Fernandes Jr., C. Peppe, R.A. Burrow, E.M. Vázquez-López, Z. Anorg. Allg. Chem. 629 (2003) 215.
[5] E. Schulz Lang, G. Manzoni de Oliveira, R.M. Fernandes Jr., E.M. Vázquez-López, Inorg. Chem. Comm. 6 (2003) 869.
[6] E. Schulz Lang, G. Manzoni de Oliveira, R.M. Fernandes Jr., E.M. Vázquez-López, Z. Anorg. Allg. Chem. 630 (2004) 717.
[7] E. Schulz Lang, G. Manzoni de Oliveira, G.N. Ledesma, Z. Anorg. Allg. Chem. 631 (2005) 1524.
[8] E.S. Schulz Lang, G.A. Casagrande, G. Manzoni de Oliveira, G.N. Ledesma, S.S. Lemos, E.E. Castellano, U. Abram, Eur. J. Inorg. Chem. 5 (2006) 958.
[9] E. Schulz Lang, G. Manzoni de Oliveira, G.A. Casagrande, J. Organomet. Chem. 691 (2006) 59.
[10] D.D. Perrin, W.L.F. Armarego, Purification of Laboratory Chemicals, third ed., Pergamon Press, 1988, p. 65.
[11] R.L.O.R. Cunha, A.T. Omori, J.V. Comasseto, J. Organomet. Chem. 689 (2004) 3631.
[12] G.M. Sheldrick, SHELXS-97, Program for Crystal Structure Solution, University of Göttingen, Germany, 1997.
[13] G.M. Sheldrick, SHELXL-97, Program for Crystal Structure Refinement, University of Göttingen, Germany, 1997.